

Microstructure and upconversion luminescence of Yb^{3+} and Ho^{3+} co-doped BST thick films

Tianjin Zhang · Lin Yu · Jingyang Wang ·
Jiqing Wu

Received: 16 March 2010 / Accepted: 20 July 2010 / Published online: 4 August 2010
© Springer Science+Business Media, LLC 2010

Abstract $\text{Ba}_{0.8}\text{Sr}_{0.2}\text{TiO}_3$ (BST) thick films co-doped with Yb^{3+} and Ho^{3+} were fabricated by the screen printing techniques on alumina substrates. The structure and morphology of the BST thick films were studied by XRD and SEM, respectively. After sintered at 1240 °C for 100 min the BST thick films are polycrystalline with a perovskite structure. The upconversion luminescence properties of the RE-doped BST thick films under 800 nm excitation at room temperature were investigated. The upconversion emission bands centered at 470 and 534 nm corresponding to $^5\text{F}_1 \rightarrow ^5\text{I}_8$ and $^5\text{F}_4 \rightarrow ^5\text{I}_8$ transition, respectively were observed, and the upconversion mechanisms were discussed. The dependence of the upconversion emission intensity upon the Ho^{3+} ions concentration was also examined; the emission intensity reaches a maximum value in the sample with 2 mol% Yb^{3+} and 0.250 mol% Ho^{3+} ions. All the results show that the BST thick films co-doped with Yb^{3+} and Ho^{3+} may have potential use for photoelectric devices.

Introduction

Recently, the interest in upconversion emission in RE-doped materials has been greatly increased because of the search for all solid-state compact laser devices operating in the visible region and the availability of powerful nearinfrared laser diodes. The potential applications include detection of infrared radiation by converting infrared signals into the visible light and upconversion lasers [1–4].

In order to investigate new upconversion materials with high luminescence efficiency, hosts with low phonon energies are required. The advantage of sulfide- and chloride-based hosts over the most extensively studied fluoride compounds is the lower phonon energy that leads to a significant reduction of the multiphonon relaxation rates. This allows an increased lifetime of some excited levels that can relax radiatively or can store energy for further upconversion, cross relaxation, or energy-transfer processes [5–9]. Unfortunately, one drawback of sulfide and chloride systems is that these materials usually present poor mechanical properties, moisture sensitivity, and are difficult to synthesize. Compared to the materials above, rare earth doped barium strontium titanates have been studied as a promising host because of its perfect electronic and electro-optic properties, strong mechanical properties, and easy incorporation of rare earth ions [10, 11].

Yb^{3+} sensitized upconversion energy transfer is especially attractive, because Yb^{3+} and Ho^{3+} upconversion energy transfer is relatively simple compared to upconversion involving other rare-earth ions. In the previous reports, Yb^{3+} and Ho^{3+} co-doped materials have been extensively investigated in a variety of glasses and crystals [12–17]. But there are few articles about the upconversion emission of Yb^{3+} and Ho^{3+} co-doped BST thick films. In this work, we investigated the influence of Yb^{3+} and Ho^{3+} on the microstructure of $\text{Ba}_{0.8}\text{Sr}_{0.2}\text{TiO}_3$ (BST) thick films, and the upconversion luminescence of RE-co-doped BST thick films was measured and discussed as well.

Experiment procedure

The RE-doped BST powders were prepared by the conventional solid phase method using barium carbonate

T. Zhang (✉) · L. Yu · J. Wang · J. Wu
School of Materials Science and Engineering, Hubei University,
Wuhan 430062, People's Republic of China
e-mail: zhangtj@hubu.edu.cn

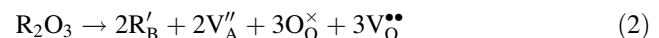
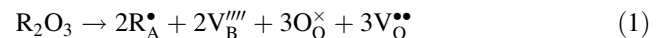
(BaCO₃, 99.9%), strontium carbonate (SrCO₃, 99.9%), titanium dioxide (TiO₂, 99.9%), ytterbium oxide (Yb₂O₃, 99.99%) and holmium oxide (Ho₂O₃, 99.99%) as starting materials. The BST thick film paste was prepared by mixing the BST powders (70 wt%) with organic vehicle(30 wt%). The prepared thick film pastes were then screen printed onto a 96% alumina substrate. Then, the printed patterns were kept at 450 °C for 30 min to remove the organic solvents and then annealed at 1240 °C for 100 min in oxygen atmosphere for crystallization. A set of samples with 2 mol% Yb³⁺ and varying Ho³⁺ concentrations of 0.100, 0.125, 0.250, 0.400, and 1.000 mol% were prepared.

The film crystal structures were examined using X-ray diffraction (XRD, Rigaku D/Max-IIIC) with Cu K α radiation ($\lambda = 1.5406 \text{ \AA}$) at 35 kV, 25 mA and a scanning speed of 6°/min. Surface morphology of Yb³⁺ and Ho³⁺ co-doped BST thick films was analyzed by scanning electron microscope (NOVA Nano 400). Upconversion luminescence spectra of the films were measured by fluorospectrophotometer (Hitachi RF-540) under 800 nm excitations from a laser diode. All the measurements were carried out at room temperature.

Results and discussions

Figure 1a shows the XRD patterns of BST thick films with various Ho³⁺ concentrations which were deposited on alumina substrates and sintered at 1240 °C. All BST thick films are polycrystalline with a perovskite structure. For further discussion, the (200) peaks of five samples are chosen to investigate the influence of Yb³⁺ and Ho³⁺ co-doping on the structures of the BST films. It can be seen from Fig. 1b that when the Ho³⁺ concentrations are increased from 0.100 to 0.250 mol%, the (200) peaks shift

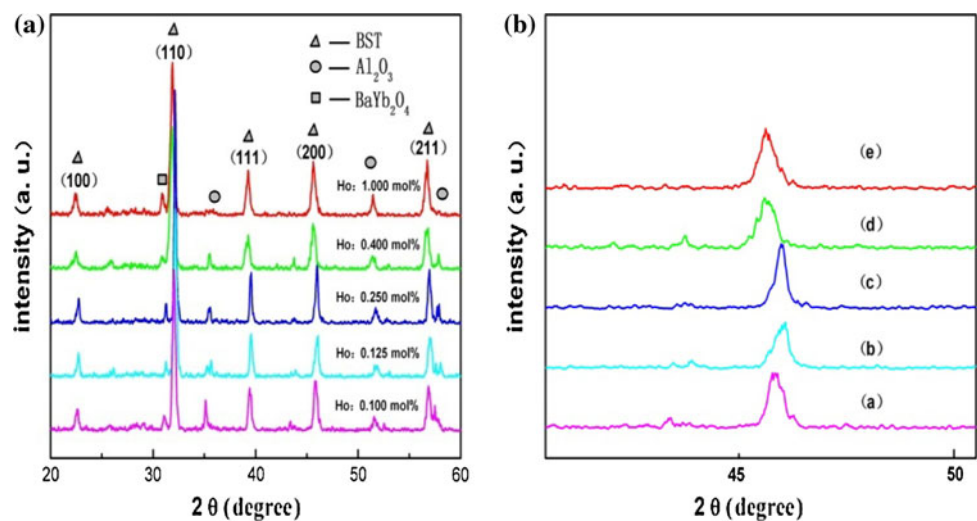
toward higher diffraction angles, but when the Ho³⁺ concentrations are increased from 0.250 to 1.000 mol%, the peaks shift toward low diffraction angle slightly. It indicates that the lattice parameters decrease as Ho³⁺ concentrations are increased from 0.100 to 0.250 mol%, but slightly increase when Ho³⁺ concentrations are increased from 0.250 up to 1.000 mol%. The reason is that Yb³⁺ and Ho³⁺ ions can substitute A site and/or B site ions in ABO₃ structure. The ionic radii of Yb³⁺, Ho³⁺, Ba²⁺, Sr²⁺, and Ti⁴⁺ are 0.99, 0.98, 1.35, 1.13, and 0.68 Å, respectively. When the Ho³⁺ concentrations are increased from 0.100 to 0.250 mol%, Yb³⁺ ions and Ho³⁺ ions mainly substitute A site (Ba²⁺, Sr²⁺) ions. It leads to decrease of the lattice parameter. But when Ho³⁺ concentrations increase from 0.250 mol% to 1.000 mol%, Yb³⁺ ions and Ho³⁺ ions substitute both A site (Ba²⁺, Sr²⁺) ions and B site (Ti⁴⁺) ions in the BST structure, so the lattice parameter increase [18]. On the other hand, the presence of oxygen vacancies owing to the ions substitution also increases the lattice parameter of the thick films. The defect equations are following [19].



where R represents a 3+ rare-earth cation, O represents a 2- oxygen anion, R_A[•] represents a 1- rare-earth anion arising from a rare-earth cation substituting a A site (Ba²⁺, Sr²⁺) ion, V_B^{'''} represents a 4- B site (Ti⁴⁺) vacancy, O_O[×] represents a oxygen atom, and V_O^{••} represents a 2+ oxygen vacancy. Therefore, the increase of lattice parameter with Ho³⁺ concentrations increase from 0.250 to 1.000 mol% may be related to the variation of the concentration of oxygen vacancies [20].

The surface morphologies of the Yb³⁺ and Ho³⁺ co-doped BST thick films were evaluated using SEM, as

Fig. 1 **a** X-ray diffraction patterns of Yb³⁺ and Ho³⁺ co-doped BST thick films; **b** The (200) peaks of Yb³⁺ and Ho³⁺ co-doped BST



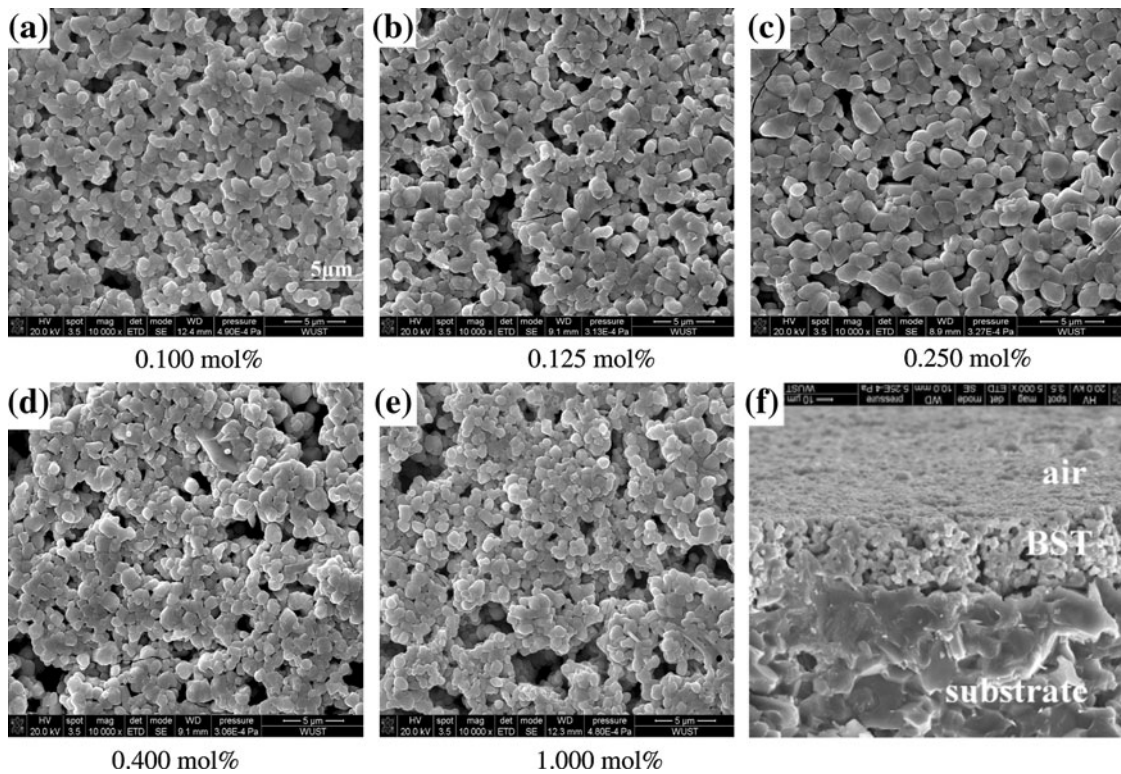


Fig. 2 SEM images of the BST thick films co-doped with 2 mol% Yb^{3+} and different Ho^{3+} concentrations

shown in Fig. 2a–f. It can be seen that all the BST thick films were uniform. Nevertheless, the Yb^{3+} and Ho^{3+} co-doping leads to noticeable changes on the surface morphology. Seeing from the Fig. 2a–e, the average grain size increase with the increases of Ho^{3+} concentrations from 0.100 to 0.250 mol%. Then the grain size decreases when the Ho^{3+} concentrations are further increased. The reason is that the growth of grains is restrained by superfluously doped ions in grain boundary. The 2 mol% Yb^{3+} and 0.250 mol% Ho^{3+} co-doped BST film has the largest grain size and density among the samples. The average grain size is about 0.2–0.3 μm and the thickness of the films is approximately 10 μm (see Fig. 2f).

Upconversion luminescence spectra of BST thick films were measured under the excitation laser photon wavelength (800 nm) at room temperature, as shown in Fig. 3. The band corresponding to the blue emission coming from the $^5\text{F}_1 \rightarrow ^5\text{I}_8$ transition is situated between 460 and 500 nm with a maximum at 470 nm. Another strong band corresponding to green luminescence coming from $^5\text{F}_4 \rightarrow ^5\text{I}_8$ transition is situated between 520 and 545 nm with maximum at 534 nm. Under 800 nm excitation, three possible approaches can populate $^5\text{F}_1$ manifold and produce upconversion blue emissions at 470 nm (see Fig. 4). (I) Excited state absorption (ESA): after a first excitation to the $^5\text{I}_5$ level, a second photon is absorbed by the same ion, exciting it to the $^5\text{F}_1$ state (see Eqs. 3 and 4); (II) Energy

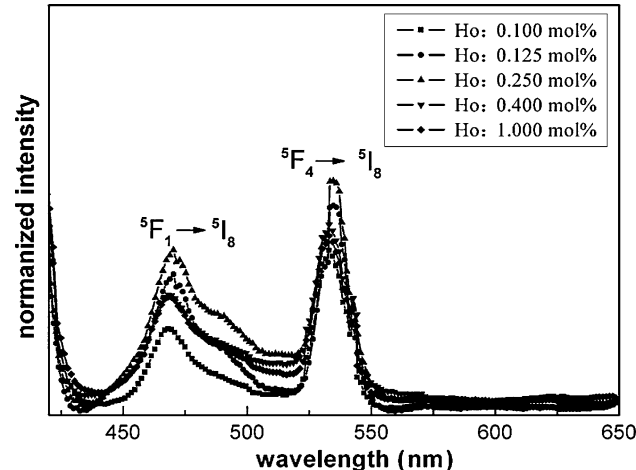


Fig. 3 PL spectra of BST thick films co-doped with Yb^{3+} and Ho^{3+} , excitation wavelength 800 nm

transfer (ET): an excited ion relaxes from $^2\text{F}_{5/2}$ state to the ground state $^2\text{F}_{7/2}$ nonradiatively and transfer the energy to another neighboring one, promoting the latter to the $^5\text{F}_1$ state from the $^5\text{I}_5$ level (see Eqs. 5, 6, and 7); (III) Energy transfer (ET): two excited ions relax from $^2\text{F}_{5/2}$ state to the ground state $^2\text{F}_{7/2}$ nonradiatively and transfers the energy to other neighboring ones, promoting the latters from $^5\text{I}_8$ to $^5\text{I}_5$ and then to the $^5\text{F}_1$ state (see Eqs. 8, 9, and 10) [21, 22].

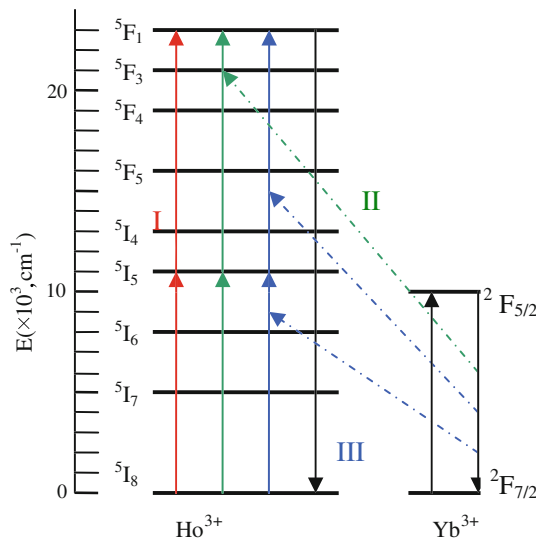
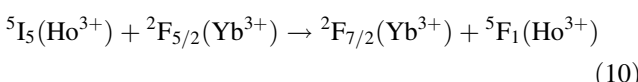
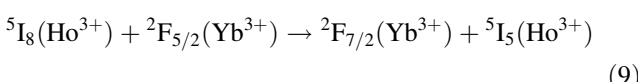
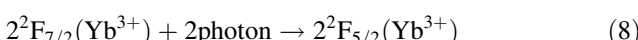
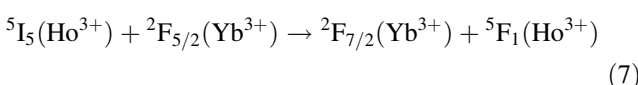
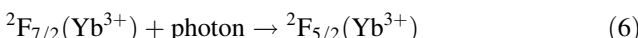
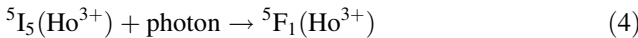
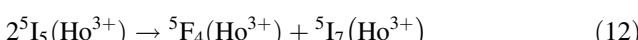
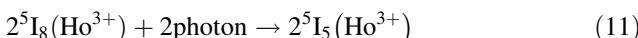


Fig. 4 Schematic diagram of ESA (I) and ET (II, III) approaches for the blue upconversion emissions under 800 nm excitation



Two possible approaches can populate the 5F_1 manifold and produce upconversion green emissions at 534 nm (see Fig. 5): (IV) Cross relaxation (CR): two same excited ions relax from 5F_5 state to the state 5I_7 nonradiatively and transfer the energy to another neighboring one, promoting the latter to 5F_4 state (see Eqs. 11 and 12); (V) Energy transfer (ET): an excited ion populated by processes (IV) is excited to the 5F_4 from 5I_7 by absorbing a photon (see Eq. 13) [23, 24].



As can be seen from the Fig. 6, the emission intensity increases as Ho^{3+} concentrations increase from 0.100 to

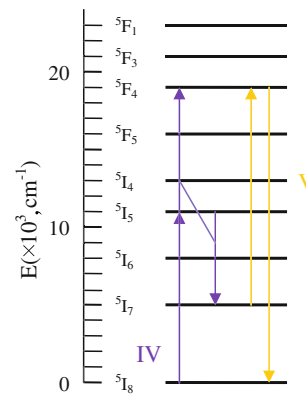


Fig. 5 Schematic diagram of CR (IV) and ET (V) approaches for the green upconversion emissions under 800 nm

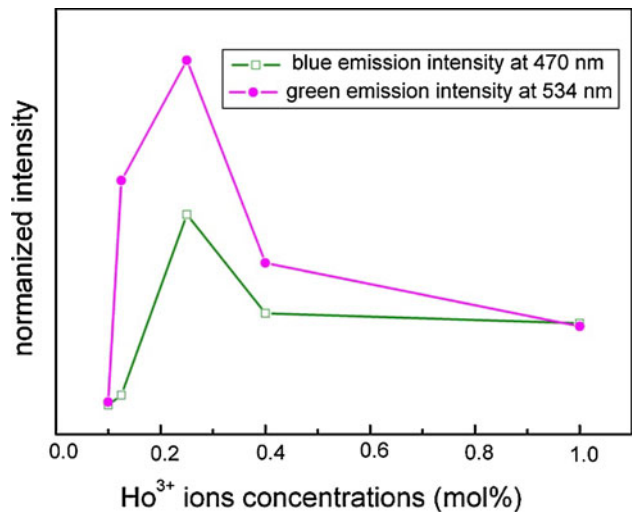


Fig. 6 The plot of intensities against Ho^{3+} ion concentrations for blue emission at 470 nm and green emission at 534 nm

0.250 mol%, and the intensity reaches a maximum value with 2 mol% Yb^{3+} and 0.250 mol% Ho^{3+} ions concentration. Then the emission intensity decreases with the increase of Ho^{3+} concentrations from 0.250 up to 1.000 mol%. The reason for this phenomenon may be that the ion pairs or clusters are formed after the Ho^{3+} doping concentrations are above 0.250 mol%. In this case, the $Ho^{3+}-Ho^{3+}$ or $Yb^{3+}-Ho^{3+}$ distances are too small in the BST lattice which may cause fluorescence quenching. The energy transfer probability for electric multipolar interactions can be generally written as [25]

$$p_{SA} = \frac{(R_0/R)^S}{\tau_S}$$

where R_0 is the critical transfer distance for which excitation transfer and spontaneous deactivation of the sensitizer (Yb^{3+}) have equal probability, τ_S is the actual lifetime of

the sensitizer excited state, including multiphonon radiative decay, S is a positive integer depending on the interactions between dipoles, and R is the distance between two ions. It indicates that the value of P_{SA} will increase when the value of R decreases. Hence, the decrease of emission intensity is mainly because of the decrease of the distance of $\text{Ho}^{3+}-\text{Ho}^{3+}$.

Conclusions

Yb^{3+} and Ho^{3+} co-doped BST thick films were fabricated by the screen printing technique on alumina substrates. XRD revealed that all the BST thick films are polycrystalline with a perovskite structure, while SEM showed a crack-free uniform microstructure of the BST thick films. The 2 mol% Yb^{3+} and 0.250 mol% Ho^{3+} co-doped BST thick film has the largest grain size and density. The average grain size is about 0.2–0.3 μm and the thickness of the films is approximately 10 μm . Under 800 nm excitation, the upconversion blue and green emissions were observed. The band corresponding to the blue emission coming from the $^5\text{F}_1 \rightarrow ^5\text{I}_8$ transition is situated between 460 and 500 nm with a maximum at 470 nm. The band corresponding to green luminescence coming from $^5\text{F}_4 \rightarrow ^5\text{I}_8$ transition is situated between 520 and 545 nm with a maximum at 534 nm. The upconversion luminescence intensity reaches a maximum value in the sample with 2 mol% Yb^{3+} and 0.250 mol% Ho^{3+} ions concentration. The luminescence intensity decreases when the Ho^{3+} doping concentration increases from 0.250 to 1.000 mol%. The reason is the presence of Ho^{3+} clusters for the heavy doping concentration, which diminishes the emission intensity. All the results show that the BST thick films co-doped with Yb^{3+} and Ho^{3+} have very good luminescence properties, and show potential applications in blue or green photonic devices.

Acknowledgements This work has been supported by the National Natural Science Foundation of China through No. 50972040, and Ceramics Ministry-Province Jointly-Constructed Cultivation Base for State Key Laboratory through No. G0701.

References

- Vossler GL, Brooks CL, Winik KA (1995) Electron Lett 31:11629
- Whitley TH, Millar CA, Wyatt R, Brierley MC, Szebesta D (1991) Electron Lett 27:1785
- Roman JE, Camy P, Hempstead M, Brocklesby WS, Nouth S, Beguin A, Lerminiaux C, Wilkinson JS (1995) Electron Lett 31:1345
- Pollack A, Chang DB (1988) J Appl Phys 64:2885
- Kaminskii AA (1996) Crystalline lasers: physical processes and operating schemes. CRC Press, New York
- Gudel HU, Pollnau M (2000) J Alloys Comp 303–304:307
- Bowman SR, Shaw LB, Feldman BJ, Ganem J (1996) IEEE J Quantum Electron 32:646
- Page RH, Schaffers KI, Payne SA, Krupke WF (1997) J Light-wave Technol 15:787
- Basiev TT, Orlovskii YuV, Galagan BI, Doroshenko ME, Vorob'ev IN, Dmitruk LN, Papashvili AG, Skvortsov VN, Konyushkin VA, Pukhov KK, Ermakov GA, Osiko VV, Prokhorov AM, Smith S (2002) Laser Phys 12:859
- Garcia-Adeva AJ, Balda R, Fernandez J, Nyein EiEi, Hommerich U (2005) Phys Rev B 72:165116
- Zhang HX, Kam CH, Zhou Y, Han XQ, Buddhudu S, Xiang Q, Lam YL, Chan YC (2000) Appl Phys Lett 77:5
- Solarz P, Sokoska I, Ryba-Romanowski W (2002) J Mol Struct 614:325
- Suyver JF, Kik PG, Kimura T, Polman A, Franzo G, Coffa S (1999) Nucl Instrum Methods Phys Res B 148:497
- Terasako T, Hashimoto K, Nomoto Y, Shirakata S, Isomura S, Niwa E, Masumoto K (2000) J Lumin 87(89):1056
- Lee YC, Shu HT, Shen JL, Liao KF, Uen WY (2001) Solid State Commun 120:501
- Zaldo C, Martin MJ, Sole R, Aguiló M, Diaz F, Roura P, de Miguel MLopez (1998) Opt Mater 10:29
- Karmakar B (2005) J Solid State Chem 178:2663
- Zhang Tj, Wang J, Jiang J, Pan Rk, Zhang Bsh (2007) Thin Solid Films 515:7721
- Zhang J, Zhai J, Chou X, Yao X (2008) Mater Chem Phys 111:409
- Wu HK, Barnes FS (1998) Integr Ferroelectr 22:291
- Liu FS, Liu QL, Liang JK, Luo J, Yang LT, Song GB, Zhang Y, Wang LX, Yao JN, Rao GH (2005) J Lumin 111:61
- Chen X, Song Z, Sawanobori N, Ohtsuka M, Li X, Wang Y, Xu X, He C, Ma H, Chen Y, Zhu J (2008) Phys B 403:3847
- Kuo S-Y, Chen C-S, Tseng T-Y, Chang S-C, Hsieh W-F (2002) J Appl Phys 92:4
- Balda R, Garcia-Adeva AJ, Voda IM, Fernandez J (2004) Phys Rev B 69:205203
- Auzel F (2004) Chem Rev 104(1):139